J Mater Sci (2007) 42:3994–4003
DOI 10.1007/s10853-006-0177-6

Retardation of grain growth in electrodeposited Cu by an electric field

Kang Jung · Hans Conrad

Received: 13 March 2006 / Accepted: 6 April 2006 / Published online: 31 January 2007
© Springer Science+Business Media, LLC 2007

Abstract The application of an external dc electric field E = 5 kV/cm during the annealing of electrodeposited Cu foil at 150–195 °C retarded grain growth. The time dependence of the grain size both with and without the field was

$$D = A_o \exp(-Q/RT)t^n$$

where A_o = (3.53–4.35) × 10^{-5} m s^{-1}, Q = 11.3–11.6 kJ/mole and n = 0.048–0.052. The field consistently reduced A_o, but had no clear effect on Q and n. Consideration of the grain growth kinetics in terms of the expression $dD/dt = M_o \exp(-Q_M/RT)P^q$ gave $Q_M = Q/n$ = 233–239 kJ/mole and $q = 1/n-1$ = 19.1–20.1. Theoretical considerations along with data in the literature on grain boundary migration in Al and Cu suggest that these values of q and Q_M could reflect the action of impurities. Several possibilities are given for the decrease in A_o and the corresponding retardation of grain growth by the field. Good accord occurred for a reduction by the field of the dislocation density contribution to the driving force P. Grain growth data in the literature, along with the present results, are in some accord with *both* the impurity drag and topology models; hence both should be considered in any analysis of grain growth kinetics.

K. Jung · H. Conrad (✉)
Materials Science and Engineering Department, North Carolina State University, Raleigh, NC 27695-7907, USA
e-mail: hans_conrad@ncsu.edu

Introduction

To obtain higher strength and/or ductility there has developed in recent years a strong interest in metals with grain size in the submicron range. However, because of the high internal energy, fine-grained metals will tend to be unstable, leading to rapid grain growth. Since in prior work [1] it was found that the application of an external dc electric field during the annealing of cold worked Al and Cu wire *retarded* recovery and recrystallization, the objective of the present investigation was to determine the effect of an electric field on grain growth in a metal with a submicron grain size. The material employed was electrodeposited Cu foil, which is used in the fabrication of electronic devices.

Experimental

The material was 18 μm thick, free-standing, electrodeposited (EP) Cu foil provided by H. D. Merchant, courtesy of Gould Electronics. The foil has the following characteristics [H. D. Merchant, private communication]: (a) a slightly elongated grain structure and a moderate ⟨220⟩ texture, (b) average midsection planar grain size D_{avg} = 0.60 μm (Fig. 1) and (c) the grains contain numerous sub-boundaries, dislocations ($\rho \approx 10^{14}\,m^{-2}$) and twins. Tensile tests after annealing at 100–250 °C indicated that the microstructure is relatively stable to ~100 °C and then softens at higher temperatures.

Specimens (37 × 7 mm^2) cut from the as-received foil were annealed without and with an external dc electric field E = 5 kV/cm for various times (separate specimens) in a silicone oil bath at 150, 170 and

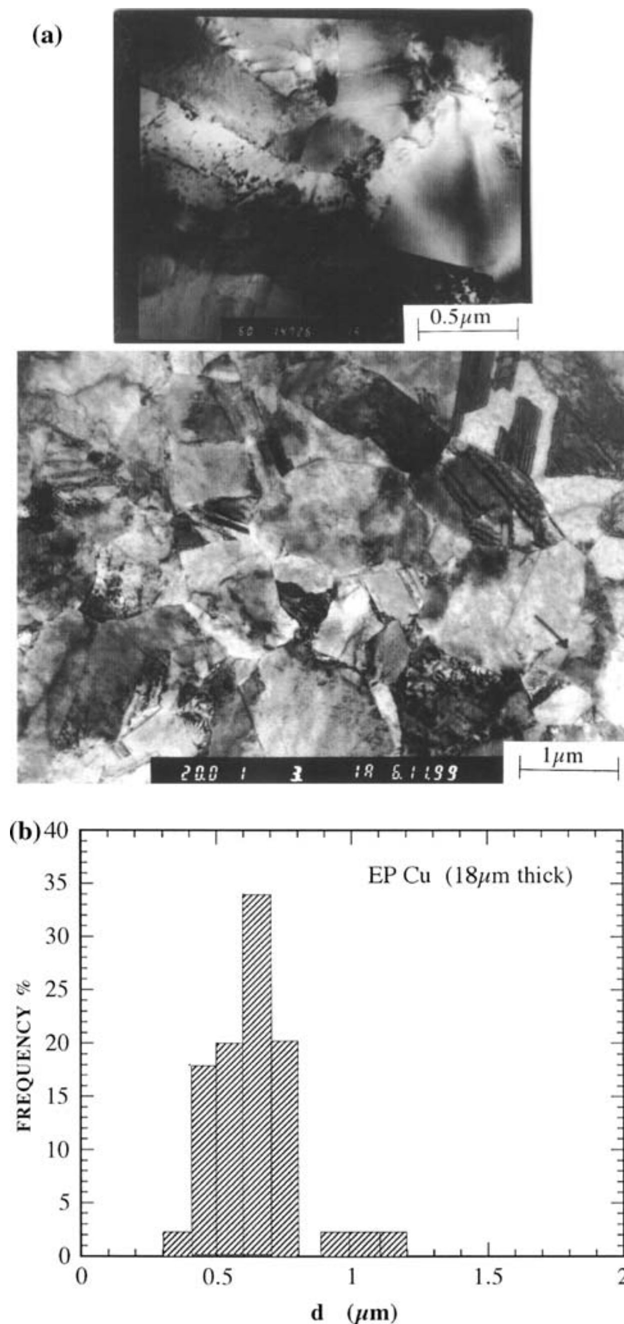

Fig. 1 (**a**) TEM micrographs at two magnifications of the EP Cu foil and (**b**) linear intercept grain size distribution of the foil. From Merchant [H. D. merchant, private communication]

195 ± 0.5 °C. The field was applied when the specimen reached the bath temperature. A schematic of the electrical arrangement is presented in Fig. 2. The electric current which occurred during annealing with the field was measured in the manner shown. Following annealing, the specimen was rinsed in ethanol and then in water prior to etching for 90 s in a solution of 10 g ammonium persulfate in 100 ml water at room temperature. The etching removed ~1.5 μm thickness from each side of the foil. The matte (top) and shiny (bottom) sides of the etched specimen were examined with a Hitachi 5-3020N scanning electron microscope (SEM) at 10,000 × magnification. The mean linear intercept grain size D was determined for each side of the foil from random lines drawn across respective micrographs.

Results

The microstructure of the top side had a cauliflower form characteristic of a columnar electrodeposited structure; the bottom had decided crystallographic features, including twin boundaries. Although the grain boundaries in both the top and bottom sides were not sharply outlined by the etch, there was nevertheless sufficient difference in the appearance of adjacent regions to permit identification of individual grains. The initial grain size D_o of the bottom side was 1.25 μm; that of the top side was 0.53 μm. These values are in accord with the grain size at the midsection determined by TEM, for which D_o ranged from 0.3 μm to 1.2 μm with D_{avg} = 0.6 μm (Fig. 1).

Log–log plots of the grain size D versus the annealing time t at the three temperatures are presented in Fig. 3a, b for the top and bottom sides of the foil, respectively. The lines give for the time-dependence of grain growth

$$D = At^n \quad (1)$$

where A increases with annealing temperature T, but decreases with electric field E, while the time exponent n is relatively independent of T and E. Making the usual assumption that the grain growth kinetics follow an Arrhenius-type behavior, expansion of Eq. 1 gives

$$D = A_o \exp(-Q/RT)t^n \quad (2)$$

where A_o is the pre-exponential and Q is an apparent activation energy. The magnitudes of n, A_o and Q obtained from a linear regression analysis of all the data are presented in Table 1. The magnitude of A_o consistently decreased with the field, but the field had no clear effect on Q and n. Similar values and trends for the three parameters were obtained from a graphical analysis of the plots of log D vs. log t, and from plots of log (dD/dt) vs. log D, where the influence of D_o is avoided.

The electric current I which occurred during the annealing of the specimens with field is shown in Fig. 4.

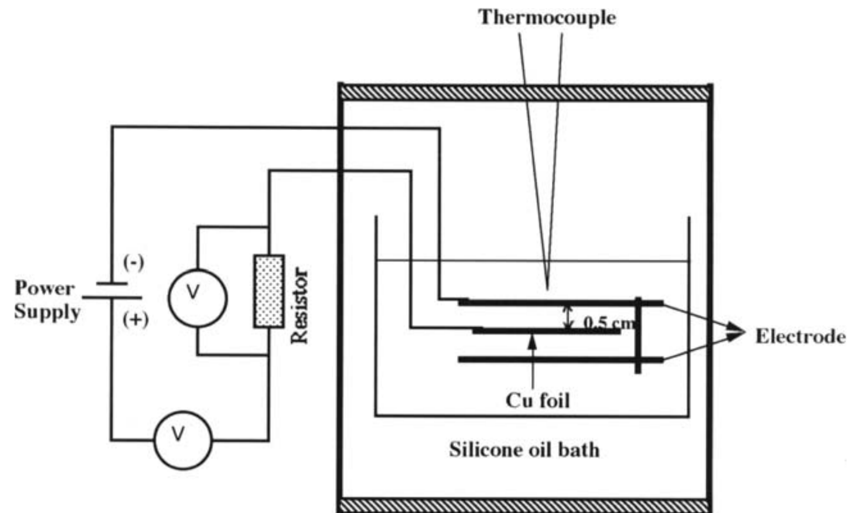

Fig. 2 Schematic of the electrical arrangement

It was of the order of μA and always initially increased slightly with time and then decreased continuously at longer times. It increased appreciably with temperature.

Discussion

Time dependence of grain growth

Grain growth during the annealing of polycrystalline metals is usually expressed by [2]

$$D^m - D_o^m = Bt = [B_o \exp(-Q^*/RT)]t \quad (3)$$

where D_o is the initial grain size, $m \geqslant 2$, B_o is the pre-exponential and Q^* the activation energy for the process. As mentioned above, the influence of D_o in any further analysis is avoided by taking the time derivative of Eq. 3, which gives

$$\mathrm{d}D/\mathrm{d}t = B/mD^{m-1} = [B_o \exp(-Q^*/RT)]/mD^{m-1} \quad (4)$$

The magnitude of the grain size exponent m can then be obtained from a plot of log(dD/dt) vs. log D. The value of m obtained from such plots for the present material was of the order of 20. Hence, for the present electrodeposited Cu, $D^m \gg D_o^m$ and Eq. 3 reduces to

$$D \approx B_o^{1/m} \exp(-Q^*/mRT) t^{1/m} \quad (5)$$

which is the equivalent to Eq. 2 with $n = 1/m$, $A_o = B_o^n$ and $Q = nQ^*$. Hence, Eq. 2 is a valid expression for the time-dependence of grain growth in the present annealing study.

Theory

Classical grain growth theories [3, 4] give for grain boundary migration velocity in a pure metal

$$V = \mathrm{d}D/\mathrm{d}t = MP \quad (6)$$

where M is the grain boundary mobility and P is the driving force, the latter being the gain in Gibbs free energy δG when a segment of the boundary having an area δA undergoes a displacement δx and thereby sweeps through a volume $\delta A \delta x$. The driving force is considered to consists of three components

$$P = P_s + P_{gb} - P_i \quad (7)$$

where P_s is the volume stored energy, P_{gb} the energy of the grain boundary and P_i that due to the presence of impurities or added solutes. P_i is usually negative, since impurities or solutes normally exert a drag on the boundary.

Dislocations, either free or contained in cells or subboundaries, are a major source of P_s. The magnitude of P_s due to free dislocations is given by [3]

$$P_{s,d} \cong \rho \mu b^2 \quad (8)$$

where ρ is the dislocation density, μ the shear modulus and b the Burgers vector. In the case of subboundaries of spacing d [5]

$$\rho_{s,s} \cong \alpha \mu b/2\pi d \quad (9)$$

where α = 1 for screw dislocations and ~3/4 for edge dislocations. The contribution of the grain boundary to P is

$$P_{gb} \cong \beta\gamma/D \quad (10)$$

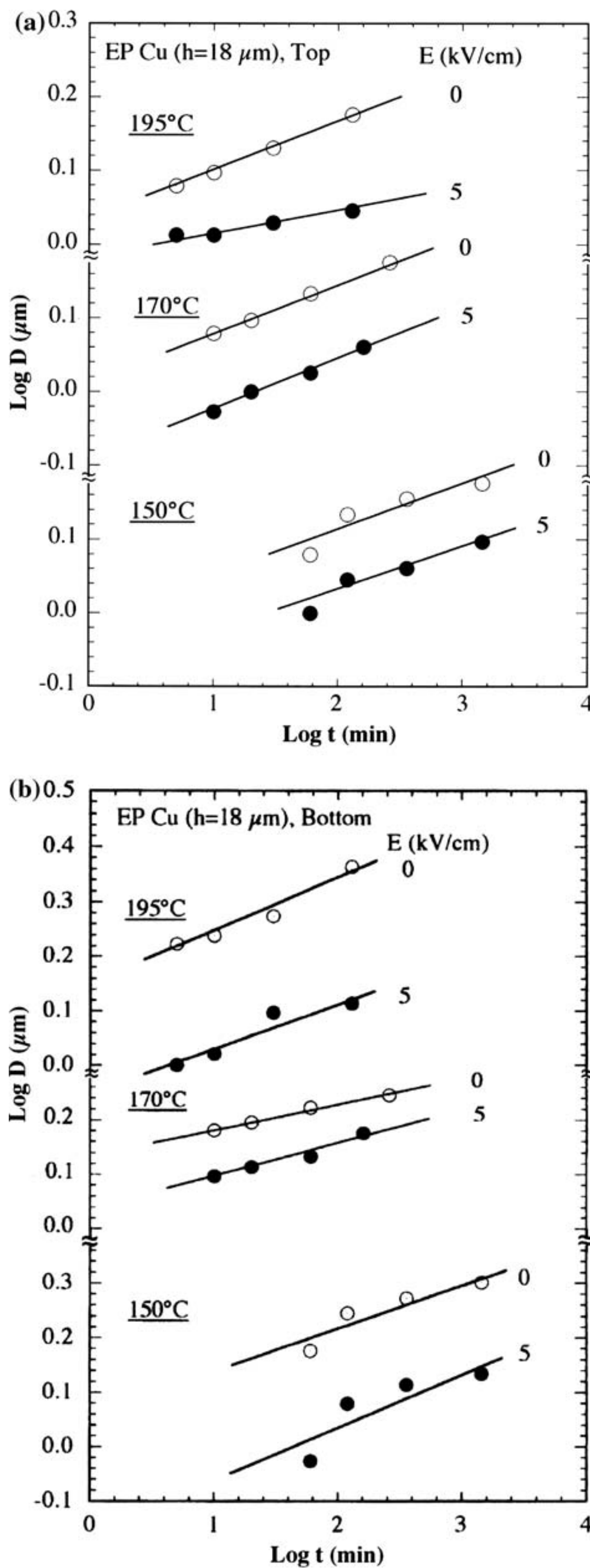

Fig. 3 Log grain size D vs. log time t for annealing at 150–195 °C (**a**) top side of foil and (**b**) bottom side

where γ is the grain boundary energy and $\beta = 2$ for three-dimensional growth [3] and 0.25 for two-dimensional grain growth [6].

In the absence of impurities or solutes grain boundary mobility is given by [3]

$$M = M_o \exp(-Q_M/RT) = \Omega D_M/kTx \quad (11)$$

where M_o is the pre-exponential and Q_M is the activation energy for the thermally activated grain boundary segment jump process. D_M is the corresponding diffusion coefficient, Ω the atomic volume and x the jump distance. When existing grain boundary vacancies are involved in the jump process, Q_M is equal to the activation energy for grain boundary diffusion Q_b. If the formation of vacancies needs to be considered, Q_M becomes that for lattice or volume diffusion Q_ℓ.

A complex relationship between V and P results with the presence of impurities or solutes. Taking into account the detailed form of the interaction energy of a solute atom with a grain boundary, Lücke and Stüwe [3] obtained the behavior shown in Fig. 5 for the variation of V with P as a function of solute concentration c. The variation of V with P according to Cahn's impurity drag theory [4] is illustrated in Fig. 6. In the low velocity region the boundary migration rate is controlled by the diffusion of the *solute* atoms perpendicular to the boundary, while in the high velocity region the diffusion of the *solvent* atoms across the boundary is controlling. Gordon and Vandermeer [7, 8] proposed that a continuous transition occurs between the low and high velocity regions, as shown in Fig. 6. The form of the curve in Fig. 6 leads to the general expression

$$V = \mathrm{d}D/\mathrm{d}t = MP^q \quad (12)$$

where $q \approx 1$ at the low and high boundary velocities and $q > 1$ at the intermediate or transition velocities.

An alternate approach to grain growth kinetics considers the topology of the grain ensemble. Employing this approach Rhines and Craig [9] developed the following expression for the time dependence of grain growth

$$1/N_v = 1/N_{v,o}[1 + M\gamma\theta\sigma t] \quad (13)$$

where N_v is the number of grains per unit volume at time t, $N_{v,o}$ the number at zero time, M the grain boundary mobility and γ the grain boundary energy. θ is a so-called ''sweeping constant'' defined as the number of grains lost when the grain boundary sweeps

Table 1 Grain growth parameters for the annealing of electrodeposited Cu at 150–195 °C without and with an electric field E

Side	E (kV/cm)	A_o (μm/s^n)	Q (kJ/mole)	n	Corr. Coeff.	$q = 1/n - 1$	$Q^* = Q/n$(kJ/mole)
Top	0	25.8	11.61	0.063	0.912	14.87	184
Bottom	0	61.2	11.51	0.041	0.915	23.39	281
Avg		43.5	11.56	0.052		19.13	232
Top	5	11.4	11.44	0.053	0.916	17.87	216
Bottom	5	59.1	11.23	0.043	0.922	22.26	261
Avg		35.3	11.33	0.048		20.07	239

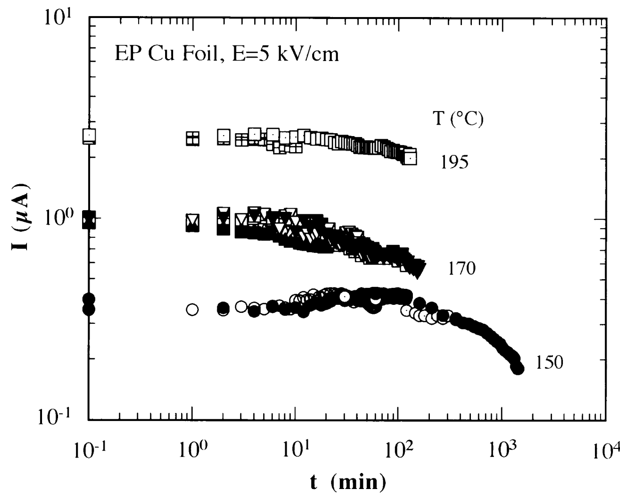

Fig. 4 Log electric current I vs. log t during the annealing with an electric field

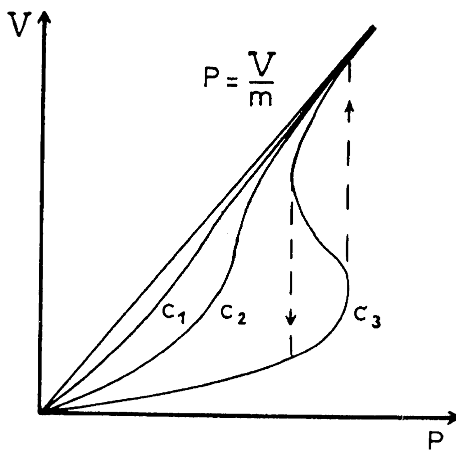

Fig. 5 Schematic of grain boundary velocity V as a function of the driving force $P = P_\gamma + P_s$ for different solute concentrations with $C_3 > C_2 > C_1$. From Lücke and Stüwe [3]

through a unit volume of material and was estimated to have a value of 4. σ is the product of the surface area times the surface curvature per grain, i.e., $\sigma = \kappa S_v/N_v$, where κ is the total surface curvature and S_v is the total surface area per unit volume. Experimentally, σ was found to be a constant. With θ and σ being constant,

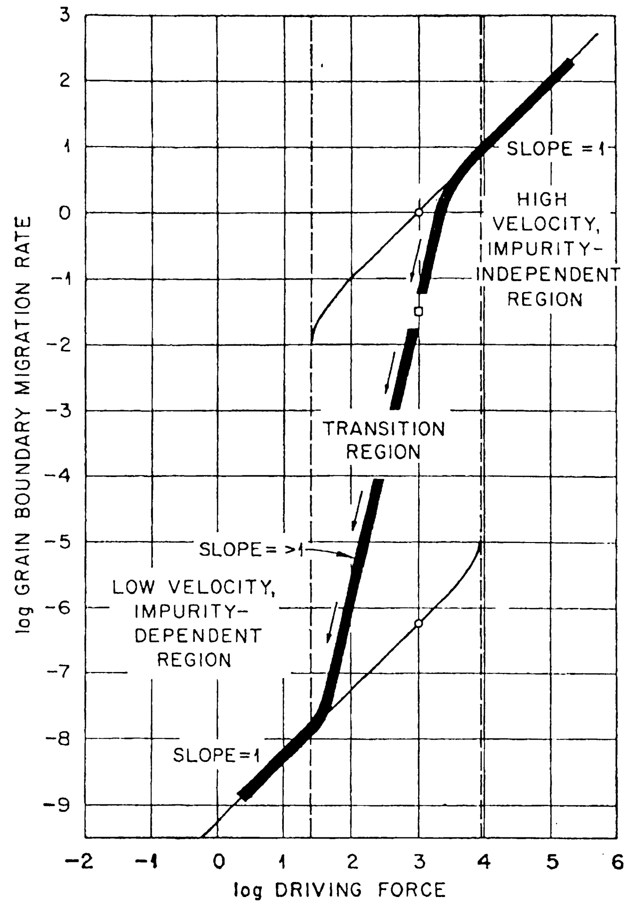

Fig. 6 Schematic of the grain boundary migration rate as a function of the driving force according to Cahn's [4] impurity drag theory. From Vandermeer [7]

Eq. 13 gives $D^3 - D_o^3 = Bt$, which is frequently found for grain growth. Equation 13 was modified by Atkinson [10] to the following expression

$$1/N_v = 1/N_{v,o} + (M\gamma\theta^*\kappa_v/N_v)t \tag{14}$$

where θ^* is the number of grains which vanish when the boundaries sweep through a volume equal to the mean grain volume $\upsilon = N_v^{-1}$, which concept had been proposed by Doherty [11].

Employing a novel Monte Carlo computer simulation procedure Anderson et al. [12] included grain

boundary topology in their treatment of grain growth. In their model the microstructure is mapped onto a discrete lattice and its temporal evaluation is monitored with respect to the shape and size of the grains. This gave microstructures similar to those of real metal specimens and gave the temperature dependence of the grain growth time exponent n shown in Fig. 7. Anderson et al. [12] proposed that experimental values of $n < 0.5$ reflect the influence of topology rather than impurities, solutes, preferred orientation or second particles, which are usually considered to be responsible.

Theoretical considerations of experimental results

Without electric field

Considering Eqs. 4, 11, and 12, one obtains

$$\frac{\mathrm{d}D}{\mathrm{d}t} = \frac{B_o \exp(-Q^*/RT)}{mD^{m-1}} = [M_o \exp(-Q_M/RT)]P^q \tag{15}$$

Taking $P_\gamma = 2\gamma/D$ gives

$$\frac{\mathrm{d}D}{\mathrm{d}t} = \frac{B_o \exp(-Q^*/RT)}{m(2\gamma)^{m-1}} P_\gamma^{m-1} = [M_o \exp(-Q_M/RT)]P^q \tag{16}$$

where according to the impurity theories $P = P_\gamma + P_s - P_i$. As pointed out by Hu and Rath [2], when $P_\gamma \gg (P_s - P_i)$ the two expressions for $\mathrm{d}D/\mathrm{d}t$ in Eqs. 15 and 16 are equivalent, giving $q = m - 1$, $Q_M = Q^*$ and $M_o = B_o/m(2\gamma)^{m-1}$, which in turn are related to A_o, Q and n of Eq. 2 when $D^m \gg D_o^m$ and Eq. 5 prevails. Further, since the dislocation density in the present EP Cu is ~10^{14} m^{-2} and the average grain size during the annealing without field is ~1.5 μm, and taking for Cu the values $\gamma = 0.65$ J/m^2, $\mu = 4.21 \times 10^{10}$ N/m^2 and $b = 2.56 \times 10^{-10}$ m, one obtains employing Eqs. 9 and 10 $P_{s,d} \approx 2.8 \times 10^5$ N/m^2 and $P_{gb} \approx 1.3 \times 10^6$ N/m^2, i.e. $P_{gb} > P_{s,d}$. The magnitude of P_i for the present material is not known.

Considering Eq. 16, and assuming that $P_\gamma \gg P_s - P_i$, the V vs. P behavior pertaining to grain growth of the present EP Cu is compared in Fig. 8 with that of other coppers [13–19] (including electrodeposits) and with measurements of grain boundary migration rate in Al [20, 21], all extrapolated to the homologous temperature $T = 0.4T_M$. Except for those from Rath and Hu [20] the data points in Fig. 8 were determined from the midrange of the results in a given reference and thus are simply typical or representative values. They include a range in impurity or solute content, measuring method, nature of the driving force and annealing temperature.

To be noted regarding Fig. 8 are the following: (a) the behavior of Cu is similar to that of Al, (b) the behavior of both Cu and Al is relatively independent of the nature of the driving force and the measuring method employed and (c) within the considerable scatter, the general behavior of both the Cu and Al resembles that shown in Fig. 6. Further, considering the present tests on EP Cu, the large value of the driving force exponent $q = 19.1$ with $E = 0$ given in Table 1 is in accord with the transition region normally ascribed to impurities. Finally, it should be mentioned that the behavior in Fig. 8 of the Cu materials with a nanometer (nc) grain size is in general accord with those having a coarser grain size.

Of further interest is a comparison of the magnitude of the time exponent n and the activation energy Q^* obtained in the prent tests on the EP Cu with those reported in the literature. Hence, n and Q^* for Al and Cu are plotted versus the homologous annealing temperature T_A/T_M in Fig. 9. Included are the results by Malow and Koch [27, 28] for Fe, since they cover a wide range in temperature (0.35–0.62T_A/T_M) and in grain size (nano to microcrystalline). Also included in Fig. 9 are the computer simulation results by Anderson et al. [12] based purely on topology considerations. It is seen in Fig. 9 that n varies from 0.05 to 0.5 and Q^* from grain boundary diffusion Q_b to lattice diffusion Q_ℓ or solute diffusion $Q_s > Q_\ell$.

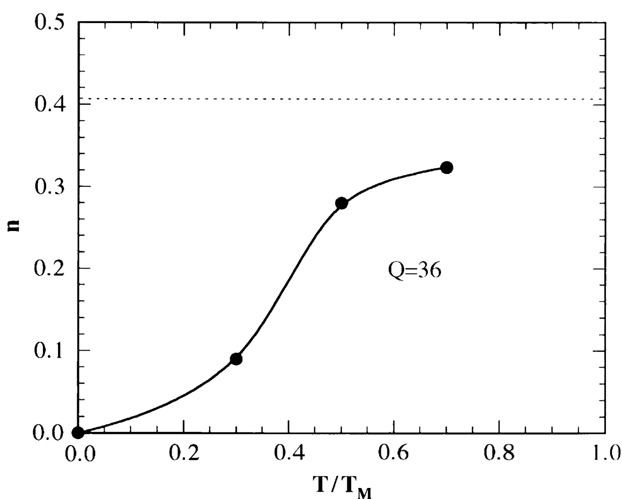

Fig. 7 Temperature dependence of the time exponent n obtained by Anderson et al. [12] from computer simulation of grain growth considering grain topology. T_M = melting temperature in K

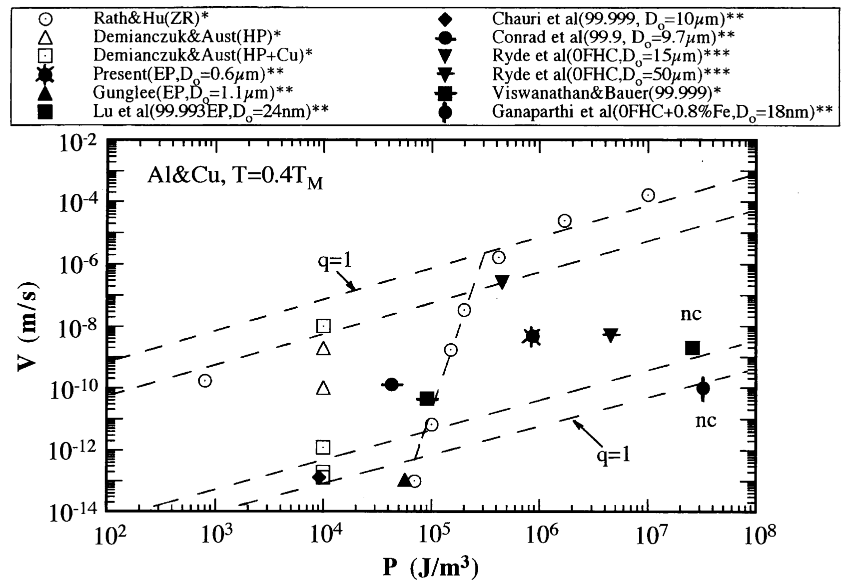

Fig. 8 Log grain boundary velocity V at $T/T_M = 0.4$ versus driving force P for Al (open symbols) and Cu (filled symbols). ZR = zone refined; HP = high purity; EP = electrodeposited; OFHC = oxygen-free, high conductivity; D_o = initial grain size. Measurement method: * = grain boundary migration, ** = grain growth, *** = recrystallization. Data from [13–21]

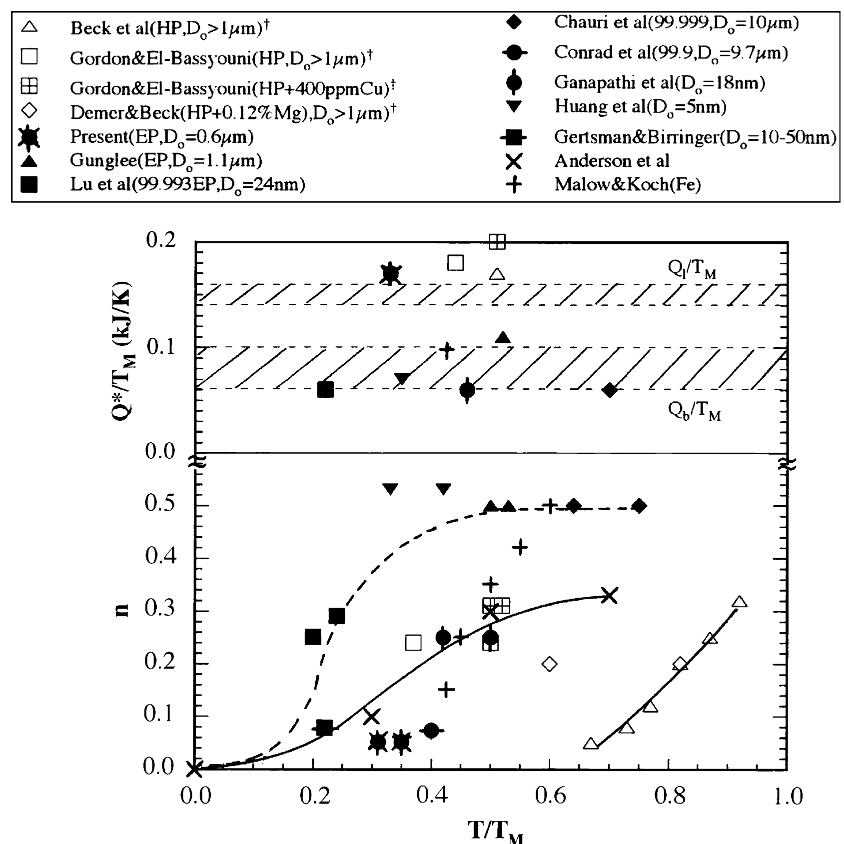

Fig. 9 The time exponent n and the normalized activation energy Q^*/T_M versus the homologous annealing temperature T/T_M. Open symbols are for Al [22–24] given in [2]; filled symbols are for Cu [present and 13, 14, 15, 17, 25, 26]; symbol + is for Fe [27, 28] and symbol × is for computer simulation based on topology [12]. The letters in the parentheses following the authors indicate the following: HP = high purity; EP = electrodeposit; D_o = initial grain size; † indicates values were taken from [2]. Activation energy for grain boundary diffusion Q_b and for lattice diffusion Q_ℓ from [29]

When considering n for different materials in Fig. 9 there is no consistent or clear variation of n with T_A/T_M. However, for a given material over a sufficiently wide temperature range n increases with temperature. Moreover, as is indicated by the results for Fe [27, 28], n does not vary with grain size from micrometers down to nanometers. Similar values and trends for n have also been reported for microcrystalline metals in general (Fig. 10 [2]) and for nanocrystalline metals and compounds (Fig. 11 [27]). Further, it should be noted that the values of n and Q^* for the present

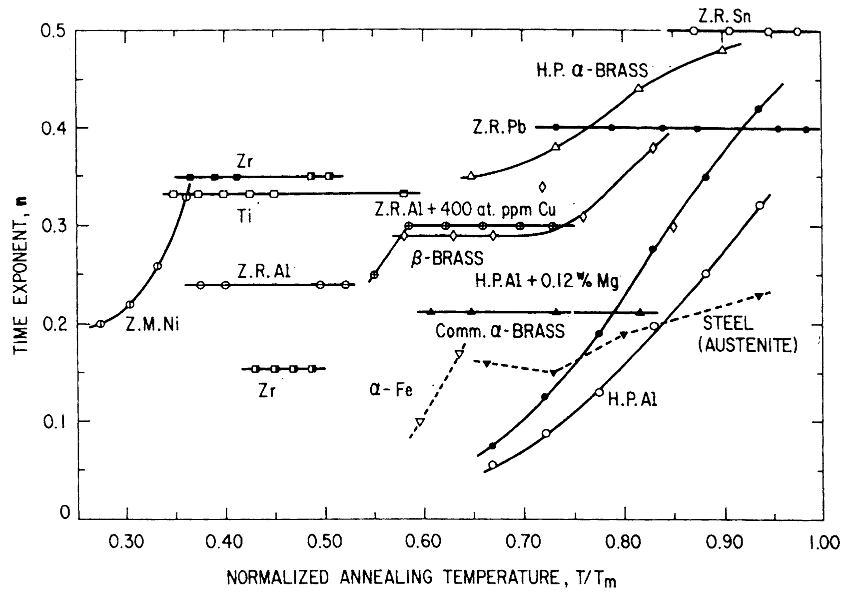

Fig. 10 Time exponent n versus homologus annealing temperature T/T_M for grain growth in various microcrystalline metals. From Hu and Rath [2]

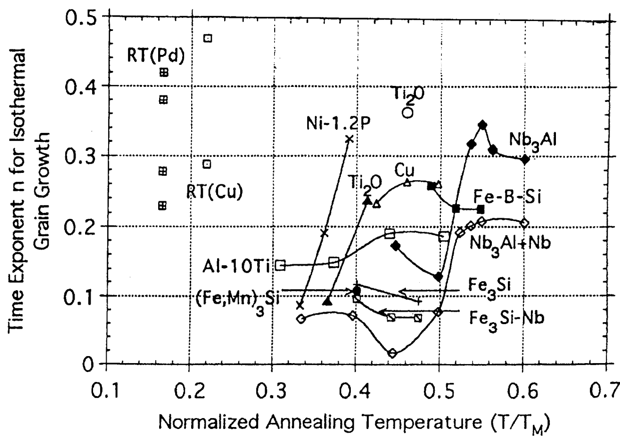

Fig. 11 Time exponent n versus homologus annealing temperature for grain growth in various nanocrystalline materials. From Malow and Koch [27]

tests on EP Cu are in accord with those obtained for metals in general and with the model by Anderson et al. [12].

Hence, the present results on EP Cu without field along with metals in general, are in some accord with both the impurity and topology models for grain growth.

It is desirable at this point to examine the degree of accord between the experimental results in Figs. 8 and 9 and the predictions of the impurity drag [3, 4] and topology theories [9, 10, 11, 12]. Although the experimental V vs. P behavior in Fig. 8 resembles that in Fig. 6 predicted by the impurity model, the resemblance is only approximate at best and in view of the large scatter cannot be taken as unambiguous confirmation of the impurity theory. Moreover, in Fig. 9 $Q^* = Q_b$ occurs for *both* small and large values of n or q (=1/n–1), rather than only for large values of n (small values of q) as predicted by Cahn's theory [4]. Thus, the data in Figs. 8 and 9 (including the present results) do not provide unquestionable confirmation of the impurity drag theories.

Regarding the topology model for grain growth, Fig. 9 shows that the experimental temperature dependence of n for grain sizes ranging from micrometers down to nanometers is in general accord with that predicted by the computer simulations of Anderson et al. [12]. Especially striking is the good agreement between the experimental temperature dependence of n for Fe [27, 28] with that predicted by the computer simulations. This accord (and that in Fig. 8) in the behavior of nanocrystalline materials with those having a much coarser grain size is in contrast to some reports [30, 31] that nanocrystalline metals have an unusually high resistance to grain growth. Malow and Koch [27] have proposed that the observed exceptionally high resistance to grain growth in nanocrystalline materials probably results from the presence of defects such as cavities, impurities and precipitates.

The above considerations indicate that grain growth in metals is in some accord with both the impurity drag and the topology models. The scatter in Figs. 8 and 9 and discrepancies often cited for either model could thus reflect that both mechanisms are concurrently operative. Therefore, in grain growth studies one needs to consider the geometry or topology of the grains as well as their size.

Grain growth with electric field

It was found in the present tests that the application of an electric field retarded grain growth rate in our electrodeposited Cu. Further, the field consistently reduced the pre-exponential A_o in Eq. 1, but had no clear effect on n or Q. A possible effect of an electric field on grain growth could be through an influence on the electronic structure of the grain boundary [32] and in turn on the grain boundary energy γ. Assuming that $P_\gamma \gg P_s - P_i$ and employing Eq. 16 with $B_o = A_o^{1/n}$ and $m = 1/n$ one obtains

$$(\gamma_E/\gamma_0)^{1-n} = (A_{0,E}/A_{0,0}) \tag{17}$$

where sub E is with field and sub-zero without. Taking $n = 0.05$, $A_{0,0} = 43.5$ μm/s^n and $A_{0,E} = 35.3$ μm/s^n from Table 1 and $\gamma_0 = 0.65$ J/m^2 one obtains $\gamma_E = 0.53$ J/m^2, which represents an 18% reduction in the grain boundary energy by the field. Whether an external electric field can give such a reduction in grain boundary energy in a metal is an open question.

Another possibility for a reduction in grain growth by the field is through a reduction in the driving force component $P_{s,d}$ due to the presence of dislocations. Support for a reduction in dislocation density by the field is provided by the decrease in flow stress and strain hardening rate which occurred during tensile tests on the present EP Cu with application of an electric field [33]. Employing Eq. 16 and assuming that $P_\gamma + P_{s,d} \gg P_i$, and that the existing dislocation density varies with D^{-1}, one obtains

$$\frac{A_{o,E}}{A_{o,o}} = \frac{P_{gb} + P_{s,d,E}}{P_{gb} + P_{s,d,o}} = \frac{P_{gb} + \rho_E \mu b^2}{P_{gb} + \rho_o \mu b^2} = \frac{35.3}{43.5} = 0.81 \tag{18}$$

where ρ_E is the dislocation density with the field, ρ_o that without and the ratio 35.3/43.5 for A_o is from Table 1. Since in general the dislocation density in metals is proportional to the square of the flow stress, we obtain from the effect of electric field on the yield stress of the present EP Cu at 150 °C in [33]

$$\frac{\rho_E}{\rho_o} = \left[\frac{\sigma_y(E)}{\sigma_y(E=0)}\right]^2 = \left[\frac{70\,\text{MPa}}{100\,\text{MPa}}\right]^2 = 0.49 \tag{19}$$

Substituting $\rho_E = 0.49\rho_o$ from Eq. 19 into Eq. 18 gives

$$\rho_o = 0.19 P_{gb}/0.32\,\mu b^2 \tag{20}$$

Taking $P_{gb} = 1.3 \times 10^6\,\text{J/m}^2 (D = 1.5\,\mu\text{m})$, Eq. 20 gives $\rho_o = 2.8 \times 10^{14}\,\text{m}^{-2}$, which is in accord with TEM measurements ($\sim 10^{14}\,\text{m}^{-2}$) on the electrodeposited Cu foils [H. D. Merchant, private communication, 34]. Moreover, taking for the tensile tests $\rho_o = \sigma_{y,o}/M\alpha\mu b)^2$ with $\sigma_{y,o} = 100\,\text{MPa}$ [33], $M = 3$ and $\alpha = 0.25$ at 150 °C one obtains $\rho_o = 1.5 \times 10^{14}\,\text{m}^{-2}$, which also is in reasonable accord with the TEM measurements and with that obtained from the grain growth results employing Eq. 20. The mechanism by which an external electric field can influence the motion of dislocations in the interior of the specimen is however not clear. To be mentioned in this regard is that in the prior work [33] it was found that the decrease in flow stress produced by an electric field increased with the charge density at the specimen surface.

Considering the topology model for grain growth, a decrease in growth rate by a field would occur if the field decreased either the parameter θ^* or κ in Eq. 14. Measurements of these topology parameters for evaluating this possibility are however lacking.

Electric current

The magnitude of the electric current shown in Fig. 4 is similar to that measured by Wu and Conrad (WC) [35] for silicone oil using Al electrodes. Onsager [36] proposed that the conductivity of dielectric liquids such as silicone oil results from the dissociation of ionic species contained therein. The activation energy Q_I obtained from the effect of temperature on the current I_o ($t = 1$ min) in Fig. 4 is 70 kJ/mole; that obtained by WC for their silicone oil at 80–150 °C was 52 kJ/mole. The difference could be due to the amount of impurities (especially H_2O) in the two oils. Whether the current had any direct influence on the grain growth kinetics is not known. It is too small (μA) for a conventional electron wind effect.

Summary and conclusions

1. The application of an external dc electric field $E = 5$ kV/cm retarded grain growth in electrodeposited Cu foil ($D_o \approx 0.6\,\mu\text{m}$) annealed at 150–195 °C.
2. The grain growth kinetics both without and with electric field were given by

   $$D = A_o \exp(-Q/RT) t^n$$

where A_o = (3.5–4.4) × 10^{-5} s^{-n}, $Q \approx$ 11.3–11.6 kJ/mole and $n \approx$ 0.048–0.052. The field consistency reduced A_o but had no clear effect on Q and n.

3. Considering the present results in terms of the expression for grain boundary migration rate $dD/dt = M_o \exp(-Q_M/RT)P^q$ gave $Q_M = Q/n = 233 - 239\,\text{kJ/mole}$ and $q = 1/n-1$ = 19.1–20.1. These values of Q_M and q are typical when impurities govern grain growth kinetics.
4. Several possibilities are given for the decrease in A_o by the field and the corresponding retardation of grain growth. Good accord occurred for a reduction by the field of the dislocation density contribution to the driving force P.
5. Grain growth data in the literature along with the present results are in some accord with both the impurity drag and topology models, indicating the need to consider both in any analysis of grain growth kinetics.

Acknowledgements This research was supported by the U.S. Army Research Laboratory and the U.S. Army Research Office under Contract No. DAA1902103 with Dr. William Mullins as contract monitor. The authors also wish to thank Dr. H. D. Merchant, Gould Electronics, Inc. for providing the electrodeposited Cu foil and Ms. R. Wolfe for typing the manuscript.

References

1. Conrad H, Guo Z, Sprecher AF (1989) Scripta Metall 23:821
2. Hu W, Rath BB (1970) Metall Trans 1:3181
3. Lücke KL, Stüwe HP (1963) In: Himinal L (ed) Recovery and recrystallization of metals. Gordan and Breach Science Publ., New York, p 171
4. Cahn JW (1962) Acta Metall 9:789
5. Cottrell AH (1853) Dislocations and plastic flow in crystals. Oxford University Press, Oxford, p 95
6. Hillert M (1965) Acta Metall 13:227
7. Vandermeer RA (1967) Acta Metall 15:447
8. Gordon P, Vandermeer RA (1966) In: Recrystallization grain growth and textures. ASM, Metal Park, p 205
9. Rhines FN, Craig KK (1974) Metall Trans 5A:413
10. Atkinson HV (1988) Acta Metall 36:469
11. Doherty RD (1975) Metall Trans 6A:588
12. Anderson MP, Srolovitz DJ, Grest GS, Sahni PS (1984) Acta Metall 32:783
13. Viswanthan R, Bauer CL (1973) Acta Metall 21:1099
14. Ghauri IM, Butt MZ, Raza SM (1990) J Mater Sci 25:4182
15. Conrad H, Guo Z, Sprecher AC (1990) Scripta Metall 24:359
16. Gangulee A (1974) J Appl Phys 45:3749
17. Lu L, Tao R, Wang LB, Ding BZ, Lu K (2001) J Appl Phys 89:6408
18. Ryde L, Hutchinson WB, Jonsson S (1990) In: Chandra T (ed) Recrystallization 90. TMS Warrendale, PA, p 819
19. Ganapathi SK, Owen DM, Chokshi AH (1991) Scripta Metall Mater 25:2699
20. Rath BB, Hu W (1969) Trans Met Soc AIME 245:1243
21. Demianczuk DW, Aust KT (1975) Acta Metall 23:1149
22. Beck PA, Kremer JC, Demer LJ, Holzworth ML (1948) AIME Trans 175:372
23. Gordon P, El-Bassyouni TA (1965) Trans TMS-AIME 233:391
24. Demer LJ, Beck PA (1949) AIME Trans 180:147
25. Huang YK, Menovsky AA, deBoer FR (1993) Nanostr Mater 2:587
26. Gertsmann VY, Birringer R (1994) Scripta Metall Mater 30:577
27. Malow TR, Koch CC (1996) In: Bourell DL (ed) Synthesis and processing of nanocrystalline powder. TMS, Warrendale PA, p 33
28. Malow TR, Koch CC (1997) Acta Mater 45:2177
29. Frost HJ, Ashby MF (1982) Deformation-mechanism maps. Pergamon Press, New York
30. Horvath S, Birringer R, Gleiter H (1987) Solid State Commun 62:319
31. Siegal KW, Ramagamy S, Hahn H, Zongquall L, Ting L, Gronsky R (1988) J Mater Sci 3:1367
32. Mauer R, Gleiter H (1985) Scripta Metall 19:1009
33. Conrad H, Yang D (2002) Acta Mater 50:2851
34. De Angelis RJ, Knorr DB, Merchant HD (1995) J Electron Mater 24:927
35. Wu CW, Conrad H (1998) J Phys D Appl Phys 31:3403
36. Onsager L (1934) J Chem Phys 2:599